

Class Incremental Learning for Adversarial Robustness

Seungju Cho*

Hongshin Lee*

Changick Kim

Korea Advanced Institute of Science and Technology

{joyga, hongsin04, changick}@kaist.ac.kr

December 7, 2023

Abstract

Adversarial training integrates adversarial examples during model training to enhance robustness. However, its application in fixed dataset settings differs from real-world dynamics, where data accumulates incrementally. In this study, we investigate Adversarially Robust Class Incremental Learning (AR-CIL), a method that combines adversarial robustness with incremental learning. We observe that combining incremental learning with naive adversarial training easily leads to a loss of robustness. We discover that this is attributed to the disappearance of the flatness of the loss function, a characteristic of adversarial training. To address this issue, we propose the Flatness Preserving Distillation (FPD) loss that leverages the output difference between adversarial and clean examples. Additionally, we introduce the Logit Adjustment Distillation (LAD) loss, which adapts the model’s knowledge to perform well on new tasks. Experimental results demonstrate the superiority of our method over approaches that apply adversarial training to existing incremental learning methods, which provides a strong baseline for incremental learning on adversarial robustness in the future. Our method achieves AutoAttack accuracy that is 5.99%p, 5.27%p, and 3.90%p higher on average than the baseline on split CIFAR-10, CIFAR-100, and Tiny ImageNet, respectively. The code will be made available.

1 Introduction

Given the susceptibility of deep neural networks to adversarial attacks, adversarial training is recognized

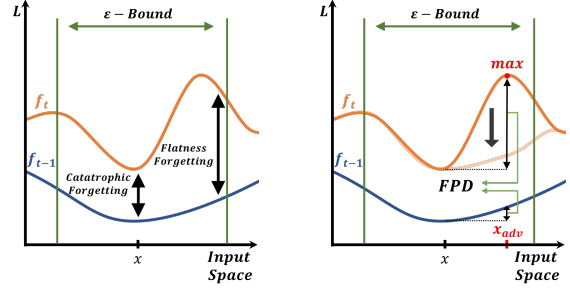


Figure 1: Illustrations of flatness forgetting problem (left) and our proposed FPD method (right). We observed a flatness forgetting problem when applying adversarial training to existing incremental learning methods. However, FPD effectively mitigates the flatness forgetting problem.

as the most effective defense method [3, 47, 44, 46]. Various approaches have contributed to enhancing adversarial training, including modifications to the overall loss function for outer minimization or the utilization of various adversarial examples for inner maximization of adversarial training [43, 50, 6, 23]. Furthermore, adversarial training has garnered significant attention not only for its role in improving adversarial robustness but also for enhancing feature representation and aiding in the interpretation of feature learning [14, 41, 40, 5, 12, 2, 26].

While adversarial training has achieved high robustness against adversarial attacks, its training and evaluation are conducted in fixed dataset settings. This constrained setting significantly diverges from real-world scenarios where trained models must continuously integrate new information. Therefore, the

integration of the incremental setting with adversarial robustness is of utmost importance, as real-world scenarios necessitate the consideration of not only malicious data but also newly incoming data [38, 8, 20, 39, 17]. Nevertheless, there is a shortage of research specifically addressing the intersection of adversarial robustness and incremental learning. In this paper, our focus is on studying adversarial robustness in class incremental learning (CIL) systems. The goal is to attain robustness against adversarially perturbed data from new classes while maintaining the previously acquired robustness from past classes. We term this task Adversarially Robust Class Incremental Learning (ARCIL).

To explore the effects of applying adversarial training in an incremental learning setup, we initially concentrate on the observations that the flatness of the loss landscape is associated with adversarial robustness [36, 35]. Consequently, we examine the input gradient and curvature of the loss function to assess the flatness. Interestingly, when we apply adversarial training to CIL methods, we observe that the flatness for the past task diminishes as models learn new tasks. As depicted in the conceptual illustration Fig. 1, adversarial training flattens the loss function (as seen in the blue line). However, after learning a new task, the flatness of the loss function is lost (as seen in the orange line). Since gradient and curvature indicate sensitivity to input changes, a large gradient and curvature mean models are vulnerable to adversarial attacks. Therefore, it is crucial to maintain the flatness acquired from adversarial training. Given that the loss function flattens and subsequently loses its flatness after learning a new task, we term this phenomenon the *flatness forgetting* problem.

To address the flatness forgetting problem, we leverage nearby data to maintain flatness on past tasks. We notice in Fig. 1 that the output difference between adversarial and clean images is related to flatness. For instance, in the blue line, the loss difference between the adversarial and the original image remains small and flat, while in the orange line, the difference is large and not flat. Therefore, we introduce *Flatness Preserving Distillation* (FPD), which preserves the subtraction of the output of a clean image and its adversarial image between differ-

ent tasks. In other words, FPD helps align the output differences between a previous model and the current model to preserve flatness. We show that FPD significantly mitigates the flatness forgetting problem, outperforming baseline.

Besides distilling flatness, we also utilize the basic distillation technique, /ie, distilling output, to mitigate the typical catastrophic forgetting problem as in [38, 24, 13]. However, distillation that transfer knowledge of unseen data may hinder the model’s adaptability to new task. Therefore, we slightly modify the output of the prior model when transferring the knowledge of the unseen data or new task’s data. Motivated by the observation that features can be categorized into robust and non-robust features [22, 6], we adjust the past model’s logit based on the robustness of the feature. Since we distill these modified logits, we refer to this approach as *Logit Adjustment Distillation* (LAD). LAD modifies the knowledge about new data that the past model has not seen, thereby enhancing the model’s adaptability to the new task.

In summary, our contributions are as follows:

- We address the less well-studied Adversarially Robust Class Incremental Learning (ARCIL) task, which involves adversarial training on sequential data.
- In ARCIL, we identify the flatness forgetting problem and propose a novel solution called Flatness Preserving Distillation (FPD) to mitigate this issue.
- By slightly modifying the outputs of previous tasks through Logit Adjustment Distillation (LAD), we enhance the model’s adaptability to new tasks.
- We assess the performance of current CIL methods in ARCIL setting and outperform their results with our proposed method, achieving superior performance in both adversarial robustness and clean accuracy.

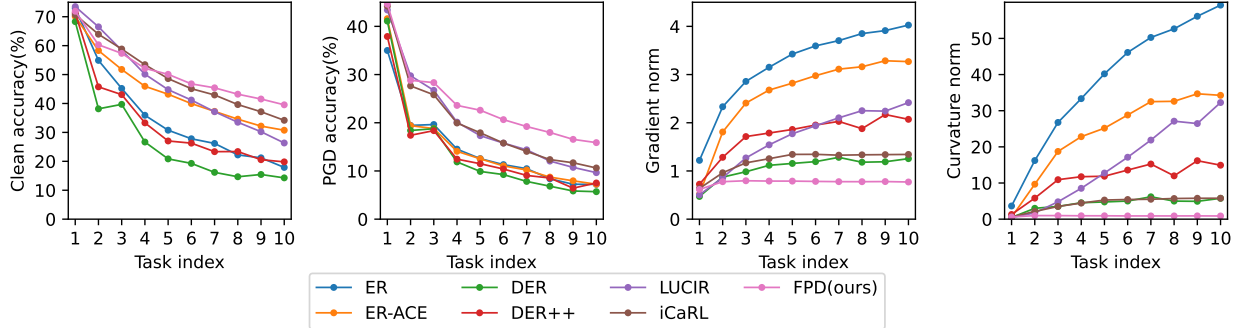


Figure 2: The experimental results for various ARCIL-revised baselines and FPD using the split CIFAR-100 dataset in incremental task steps. Four metrics are considered: clean accuracy (*Left*), 20 steps of PGD accuracy (*Middle left*), gradient norm in input space (*Middle right*), and curvature norm in input space (*Right*). Gradient and curvature norms are related to the flatness of loss in input space, with lower norms indicating better flatness. The baseline methods exhibit significant forgetting regarding clean accuracy, robustness, and flatness. In contrast, the proposed FPD method effectively preserves all of these aspects with a substantial margin.

2 Related work

We review adversarial training and incremental learning in image classification in this section.

2.1 Adversarial Training

Adversarial training makes the model robust through the following min-max problem.

$$\min_{\theta} \mathbb{E}_{(\mathbf{x}, y) \sim D} \left(\max_{\delta \in [-\epsilon, \epsilon]} [l_{obj}(\mathbf{x} + \delta, y; \theta)] \right), \quad (1)$$

where D is a data distribution over pairs of examples \mathbf{x} and corresponding labels y , θ is model parameters, l_{obj} is an objective function such as cross-entropy loss, and ϵ is a pre-defined maximum boundary. In this way, the model continues to create the worst attack that is difficult for the model to learn in an online manner during training and is strengthened by properly classifying difficult samples again. Most adversarial training uses a multi-step based Projected Gradient Attack (PGD) [33] to solve the inner maximization problem, and several regularization losses have been proposed to solve the inner minimization problem of Eq. (1).

Representatively, TRADES[49] incorporates the KL divergence loss between the output of clean an adversarial images, and MART[45] introduces per-sample weights through the confidence of each sample. Additionally, various techniques, such as data augmentation [37, 30] and knowledge distillation [16, 52, 51, 34, 21], have been proposed to improve the performance of adversarial training. However, adversarial training has been mainly dealt with only in situations in which all data are given, and there are few studies in incremental settings in which data are sequentially received. Our research explores methodologies for training a model to be adversarially robust when data is presented incrementally.

2.2 Class Incremental Learning

Class incremental learning operates under the assumption that data from new, non-overlapping classes is given sequentially rather than all at once. The distribution shift in CIL leads to a phenomenon known as *catastrophic forgetting*[17]. Consequently, the primary goal of CIL is to effectively learn new data without forgetting the knowledge acquired from the previous training. Many studies have been proposed to achieve this goal, such as utilizing knowledge

distillation [38, 31], regularization [31, 27, 42, 48], or memory buffer [38, 8, 20, 39, 9]. Among them, the memory buffer-based method, *i.e.* rehearsal method, has become a standard method to prevent forgetting since it can be combined with other methods and is effective [38, 8, 39, 20, 9]. There is also non-rehearsal methods that do not exploit memory, but these are known as not effective for complex problems [7, 1, 15]. In particular, in the case of non-rehearsal-based methods, we find that the performance is highly deteriorates when applying adversarial training.

While many CIL methods have been proposed to learn new things while effectively preventing forgetting, there remains a gap in research focusing on scenarios involving perturbed data. Recently, a study dealing with adversarial robustness from the perspective of continuous learning has been proposed, but a simple data augmentation is used [4]. In contrast, we carefully investigate whether forgetting occurs from a robust perspective.

3 Method

3.1 Problem formulation

A model f undergoes sequential training on a set of tasks $1, 2, \dots, T$, and we denote f_t as the model trained on task t for simplicity. In each individual task t , input $\mathbf{x} \in \mathbb{R}^d$ and its corresponding ground truth $y \in \mathbb{R}$ are independently and identically drawn from the task-specific data distribution $D_t = \{X_t, Y_t\}$, where $D_i \cap D_j = \emptyset$ for $i \neq j$. Here, X_t and Y_t are the set of inputs and true labels of task t . We adopt the rehearsal buffer-based approach, utilizing limited memory of past data, as proposed in prior works such as [38, 8, 39, 20]. The rehearsal buffer is denoted as $B_t \subset \cup_{i=1}^T D_i$, and we update a simple sampling algorithm after training on each task as in [38]. Note that the total exemplar size does not exceed a certain amount throughout all tasks, *i.e.*, $|B_t|$ is fixed throughout the entire training process. To merge instances from both current and previous tasks, we concatenate the buffer at the beginning of each incremental task on the current dataset, denoted

as $D_t \cup B_{t-1}$.

As we learn each non-overlapping task continuously, our goal is to achieve robustness in the new task while maintaining the robustness learned in the previous task. In the next section, we apply naive adversarial training to class incremental learning methods and present our approach.

3.2 Adversarial training with incremental learning

We first examine adversarial robustness by applying adversarial training to existing incremental learning methods. Specifically, we employ the PGD attack with ten steps to approximate inner maximization and utilize CIL methods for solving outer minimization on Eq. (1). The application of adversarial training results in an enhanced robust accuracy on the current task data. However, we concurrently observe a reduction in the robust accuracy of previously learned tasks as new tasks are introduced, as depicted in the middle left of Fig. 2.

We investigate this robustness forgetting problem in more detail. We calculate the gradient and curvature of the loss with respect to the inputs of test data from D_t after training task t as follows.

$$\begin{aligned} & \|\nabla l(f(\mathbf{x}), y)\|^2, \\ & \left\| \frac{\nabla l(f(\mathbf{x} + \mathbf{h}), y) - \nabla l(f(\mathbf{x}), y)}{\mathbf{h}} \right\|^2, \end{aligned} \quad (2)$$

where l is the loss function. The first expression refers to the gradient norm, while the second expression represents the curvature norm. Here, we estimate curvature as a finite difference using \mathbf{h} with a sufficiently small value that has the same dimension of \mathbf{x} as in [35]. In Fig. 2, we observe that the gradient and curvature increase as models learn new tasks. Although the degree of increase is different between methods, we can see that the gradient and curvature continuously increase in all of them. In the next section, we elucidate our approach to mitigating the flatness forgetting problem.

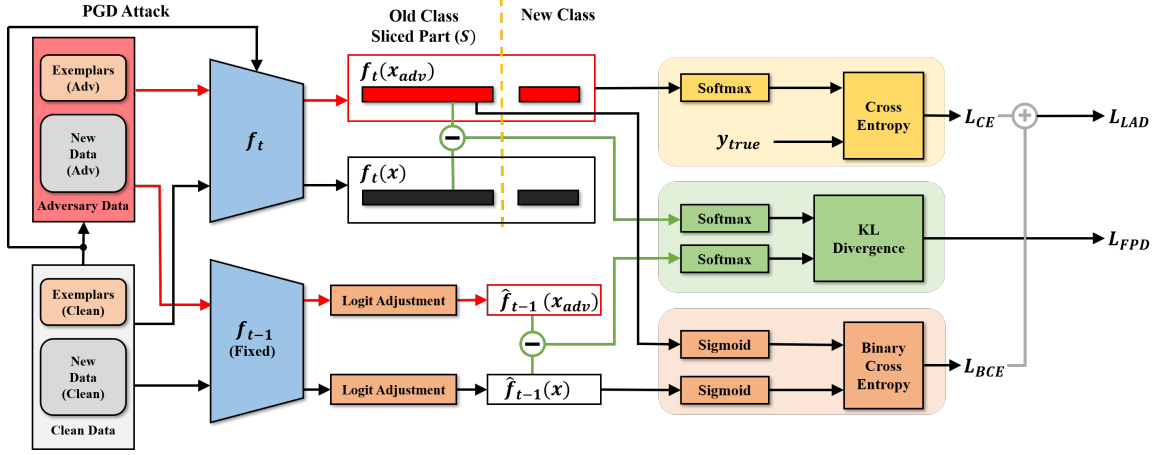


Figure 3: Main model architecture. The green part is FPD which mitigates the flatness forgetting problem, and the yellow and orange parts are LAD.

3.3 Flatness Preserving Distillation

For a clean input \mathbf{x} from the data of the current dataset $D_t \cup B_{t-1}$, the adversarial perturbed input is given by:

$$\mathbf{x}_{adv} = \mathbf{x} + \boldsymbol{\delta}. \quad (3)$$

Here, $\boldsymbol{\delta}$ represents the adversarial perturbation of the current task model. For a small perturbation $\boldsymbol{\delta}$, the output of \mathbf{x}_{adv} given the t -th task model f_t can be approximated using Taylor expansion through the input space.

$$f_t(\mathbf{x}_{adv}) = f_t(\mathbf{x}) + \nabla f_t(\mathbf{x})^T \boldsymbol{\delta} + \frac{1}{2} \boldsymbol{\delta}^T \mathbf{H}_t \boldsymbol{\delta} + O_t(\|\boldsymbol{\delta}\|^2), \quad (4)$$

where $\nabla f_t(\mathbf{x}) \in \mathbb{R}^d$ is the gradient of the t -th task model, $\mathbf{H}_t \in \mathbb{R}^{d \times d}$ is the hessian matrix of the t -th task model, and O_t stands for high order term. Similarly, the output of the $(t-1)$ -th task model can also be approximated using Taylor expansion given the t -th task input \mathbf{x}_{adv} :

$$f_{t-1}(\mathbf{x}_{adv}) = f_{t-1}(\mathbf{x}) + \nabla f_{t-1}(\mathbf{x})^T \boldsymbol{\delta} + \frac{1}{2} \boldsymbol{\delta}^T \mathbf{H}_{t-1} \boldsymbol{\delta} + O_{t-1}(\|\boldsymbol{\delta}\|^2), \quad (5)$$

where $\nabla f_{t-1}(\mathbf{x}) \in \mathbb{R}^d$ is the gradient, $\mathbf{H}_{t-1} \in \mathbb{R}^{d \times d}$ is the hessian matrix, and O_{t-1} is high order term of the $(t-1)$ -th task model.

To mitigate the flatness forgetting problem, the gradient and curvature of the input space should be preserved. In other words, the first-order and second-order terms in Eq. (4) should be maintained to have similar values to those in Eq. (5), which can be expressed as follows:

$$\begin{aligned} D(\nabla f_t(\mathbf{x}), \nabla f_{t-1}(\mathbf{x})) &< \eta, \\ D(\mathbf{H}_t, \mathbf{H}_{t-1}) &< \eta, \end{aligned} \quad (6)$$

where $D(\cdot, \cdot)$ represents the distance function, and η is a small value that tends towards zero in an optimal scenario. Therefore, the gradient and curvature of the t -th task model align with those of the $(t-1)$ -th task model if these conditions in Eq. (6) are satisfied. However, directly calculating the first and second-order terms leads to heavy computational overhead. Therefore, we adopt a more efficient approach by exploiting the subtraction between clean and adversarial outputs for both the t -th task and $(t-1)$ -th task, as follows:

$$\begin{aligned} \Delta f_t &\approx \nabla f_t(\mathbf{x})^T \boldsymbol{\delta} + \frac{1}{2} \boldsymbol{\delta}^T \mathbf{H}_t \boldsymbol{\delta}, \\ \Delta f_{t-1} &\approx \nabla f_{t-1}(\mathbf{x})^T \boldsymbol{\delta} + \frac{1}{2} \boldsymbol{\delta}^T \mathbf{H}_{t-1} \boldsymbol{\delta}, \end{aligned} \quad (7)$$

where $\Delta f_t = f_t(\mathbf{x}_{adv}) - f_t(\mathbf{x})$ and $\Delta f_{t-1} = f_{t-1}(\mathbf{x}_{adv}) - f_{t-1}(\mathbf{x})$. Here, we neglect the high-order

term due to the small magnitude of the perturbation δ . As a result, we can efficiently distill both the gradient and hessian information of the $(t-1)$ -th task model into t -th task model by using the difference between clean and adversarial inputs:

$$D(\Delta f_t, \Delta f_{t-1}) \approx D\left(\nabla f_t(\mathbf{x})^T \delta + \frac{1}{2} \delta^T \mathbf{H}_t \delta, \nabla f_{t-1}(\mathbf{x})^T \delta + \frac{1}{2} \delta^T \mathbf{H}_{t-1} \delta\right). \quad (8)$$

Assuming L1 distance as a surrogate loss for the distance metric, the equation can be expressed as follows:

$$\|\Delta f_t - \Delta f_{t-1}\| \approx \|(\nabla f_t(\mathbf{x}) - \nabla f_{t-1}(\mathbf{x}))^T \delta + \frac{1}{2} \delta^T (\mathbf{H}_t - \mathbf{H}_{t-1}) \delta\|. \quad (9)$$

By considering the left term as a loss, the t -th task model can optimize the right term to converge toward zero. As the constant δ is unrelated to the model outer minimization process, both $\nabla f_t(\mathbf{x}) - \nabla f_{t-1}(\mathbf{x})$ and $\mathbf{H}_t - \mathbf{H}_{t-1}$ become close to zero, which satisfies the Eq. (6). Consequently, we effectively distill the gradient and hessian of $(t-1)$ -th tasks into the t -th model, enabling the model to retain the information of the flatness. In the middle right and right side of Fig. 2, our method successfully maintains gradient and hessian.

Finally, the final *Flatness Preserving Distillation* (FPD) loss is formulated as follows:

$$L_{FPD}(\mathbf{x}; f_t, f_{t-1}) = D((\Delta f_t)^S, \Delta f_{t-1}), \quad (10)$$

where S represents a slicing operation that aligns the dimension of the t -th task and the $(t-1)$ -th task and KL divergence loss is experimentally selected as the surrogate loss for D .

3.4 Distillation of modified knowledge

Along with FPD, we utilize a cross-entropy loss and adversarial distillation loss L_{AD} to classify images as follows [16, 52, 51].

$$L_{AD}(\mathbf{x}; f_t, f_{t-1}) = L_{CE}(f_t(\mathbf{x}_{adv}), y) + L_{BCE}(f_t(\mathbf{x}_{adv}), f_{t-1}(\mathbf{x})), \quad (11)$$

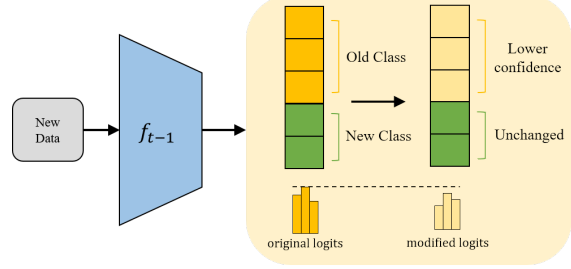


Figure 4: Diagram of LAD. We modify the logits of the old model f_{t-1} over the unseen data.

where the first term is classification loss and the second term is the distillation loss, and we choose binary cross entropy loss as in [38]. Note that in the second term, since we have a limited memory of exemplars, we adopt current data D_t with exemplars B_{t-1} when distilling knowledge of f_{t-1} as in [38, 24, 13]. Distilling the output to the current data encourages transferring what model f_{t-1} has learned as much as possible. However, although distillation from the past model f_{t-1} helps to preserve knowledge, it might interfere with learning new tasks t , resulting in a lack of plasticity. Specifically, the past model f_{t-1} has not learned anything about the current data pair, *i.e.*, f_{t-1} has too much bias or confidence to task $t-1$. Therefore, it is essential to address unseen data carefully in the distillation process.

To reduce the confidence toward task $t-1$ when f_{t-1} receives D_t as input, we modify $f_{t-1}(\mathbf{x})$. Specifically, inspired by research showing that features are divided into robust and non-robust features [22, 32, 25], we penalize non-robust features and preserve robust features of \mathbf{x} . We preserve robustness through robust features and increase plasticity by penalizing non-robust features. We consider features with a large distance between clean and adversarial images to be non-robust features, and modify the features as follows.

$$d = \|h_{t-1}(\mathbf{x}_{adv}) - h_{t-1}(\mathbf{x})\|^2, \quad \hat{h}_{t-1}(\mathbf{x}) = h_{t-1}(\mathbf{x}) \odot e^{-\beta \cdot d}, \quad (12)$$

where h be the feature extractor of f , β is a non-negative hyper-parameter and e denotes exponential function. A large distance means that the feature re-

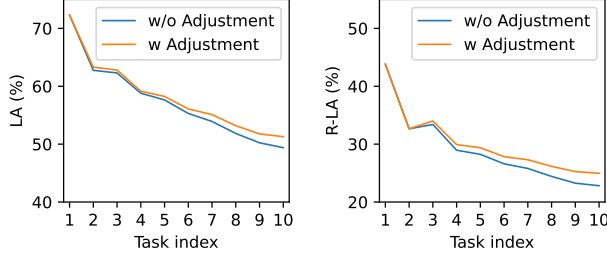


Figure 5: The learning accuracy (LA) at the end of each task t . The learning accuracy is the accuracy of task t after learning task t , *i.e.*, it measures how well the model learned the task t . The robust learning accuracy (R-LA) is the learning accuracy of adversarial examples. We utilize Split CIFAR-100 divided into ten tasks.

acts sensitively to adversarial attacks, and thus feature will be more penalized according to the large distance. Since $d \geq 0$, elements of modified feature $\hat{h}_{t-1}(\mathbf{x})$ is more smaller than that of $h_{t-1}(\mathbf{x})$, and thus reduces confidence for past tasks. We also observe that adjusting logits is helpful in learning new tasks as shown in Fig. 5, increasing plasticity. Detailed experimental settings and analyses are summarized in supplementary material.

Since we adjust logits, we name this *Logit Adjustment Distillation* (LAD) and refer to the following loss as L_{LAD} .

$$L_{LAD}(\mathbf{x}; f_t, f_{t-1}) = L_{CE}(f_t(\mathbf{x}_{adv}), y) + L_{BCE}(f_t(\mathbf{x}_{adv}), \hat{f}_{t-1}(\mathbf{x})), \quad (13)$$

where $\hat{f}_{t-1}(\mathbf{x})$ is an output after \mathbf{x} passing the logit adjustment. We summarize LAD in Fig. 4.

3.5 Overall objective function

We train the model with adversarial examples and utilize LAD and FPD. The form of our objective function is:

$$l_{obj} = L_{LAD}(\mathbf{x}; f_t, f_{t-1}) + \alpha \cdot L_{FPD}(\mathbf{x}; f_t, f_{t-1}), \quad (14)$$

where α is a hyper-parameter. Our model architecture is depicted in Fig. 3.

4 Experiments

4.1 Experimental settings

Datasets We conducted experiments with various buffer sizes on the following datasets. **Split CIFAR-10 (S-CIFAR10)** divides CIFAR-10[28] into five tasks, each consisting of two classes, with 5,000 training images in each class. **Split CIFAR-100 (S-CIFAR100)** divides CIFAR-100[28] into ten tasks, with ten classes per task, where each class consists of 500 training images. **Split Tiny ImageNet (S-TinyImageNet)** divides the Tiny ImageNet[29] into ten tasks, with 20 classes per task. Each class includes 500 training images.

Adversarial training For adversarial training, we used ten steps PGD attack with a random start for each step, and the maximum perturbation is limited to $\epsilon_\infty = 8/255$, while each step is taken with a step size of $2/255$. We implemented the adversarial training method using current CIL methods with the adversarially perturbed image for input. We conducted with ResNet-18[19] architecture in all experiments.

Evaluation We measured clean and robust accuracy after learning all incremental tasks. For evaluating robustness, we implemented 20 steps of PGD and AutoAttack (AA) [10] with $\epsilon_\infty = 8/255$. To measure forgetting on robustness, we consider the robust backward transfer (R-BWT) metric as follows.

$$\text{R-BWT} = \frac{1}{T-1} \sum_t^{T-1} (RA_{T,t} - RA_{t,t}), \quad (15)$$

where $RA_{i,j}$ denotes robust accuracy of task j after learning task i . Note that $RA_{i,i}$ is the robust learning accuracy (R-LA). Robust accuracy is calculated on 20 steps of PGD attack. Accuracy of past task usually drops as new tasks are learned, so a higher R-BWT means less forgetfulness. Note that BWT and LA are defined with the same arguments as R-BWT and R-LA, except that clean accuracy is measured for BWT and LA instead of robust accuracy.

Baselines We evaluated fine-tuning (FT) with a buffer on each dataset. FT serves as a straightforward baseline where we employ standard adversarial training using both the current task data

Dataset	Buffer Size Method	200				500				2000			
		Clean	PGD	AA	R-BWT	Clean	PGD	AA	R-BWT	Clean	PGD	AA	R-BWT
S-CIFAR10	FT w/ Buffer	28.64	18.12	17.97	-72.20	40.01	20.62	20.22	-68.45	56.87	27.24	26.50	-58.23
	R-ER	28.30	17.42	17.25	-71.91	35.14	19.01	18.86	-68.90	52.84	24.36	23.88	-57.15
	R-ER-ACE	50.86	14.38	13.84	-26.24	57.56	16.48	15.93	-31.61	66.04	20.49	19.88	-23.50
	R-DER	22.30	16.07	15.99	-64.80	27.33	16.49	16.28	-70.51	23.90	16.24	16.10	-61.45
	R-DER++	22.48	16.41	16.32	-71.94	24.14	16.53	16.43	-72.08	26.74	15.37	15.12	-69.41
	R-iCaRL	47.02	23.14	21.76	-38.20	53.61	23.95	22.73	-30.03	62.70	29.10	27.42	-23.15
	R-LUCIR	33.92	18.84	18.09	-62.75	43.41	21.47	20.17	-68.45	62.39	28.36	25.31	-30.79
	Ours	54.93	25.35	23.75	-26.25	55.76	27.59	25.62	-20.69	62.44	30.22	28.02	-15.64
S-CIFAR100	FT w/ Buffer	9.34	5.14	5.04	-41.64	12.00	5.77	5.63	-39.73	20.56	8.35	8.04	-33.26
	R-ER	9.17	4.82	4.74	-36.52	11.71	5.41	5.34	-35.16	17.18	6.48	6.30	-31.51
	R-ER-ACE	17.13	2.76	2.47	-16.67	22.70	3.67	3.31	-16.72	31.96	7.09	6.59	-14.21
	R-DER	10.65	5.22	4.64	-38.60	14.28	5.70	4.73	-37.38	17.64	7.55	6.39	-37.58
	R-DER++	10.81	5.02	4.63	-35.99	14.61	5.97	5.32	-33.69	20.51	7.15	6.47	-31.29
	R-iCaRL	24.75	7.54	6.39	-28.76	27.60	8.05	7.01	-27.58	34.89	10.78	9.26	-21.73
	R-LUCIR	14.16	6.41	5.95	-38.03	17.56	7.13	6.61	-35.24	26.05	9.62	8.90	-26.66
	Ours	31.62	12.43	9.52	-15.28	35.10	13.64	10.43	-13.47	39.44	16.59	12.69	-9.74

Table 1: Adversarial training results on S-CIFAR10 and S-CIFAR100. We measure Clean, PGD, Autoattack accuracy (%) and Robust BWT.

and the buffered data. Then, we compared our proposed method against other state-of-the-art CIL baselines listed in Table 1. Specifically, we chose ER[39], ER-ACE[9], DER/DER++[8], iCaRL[38], and LUCIR[20] as baselines. We carefully modified each loss function to fit into adversarial training and search the hyperparameters of each CIL methods. As we apply adversarial training, the baseline methods were denoted with the prefix *R*, meaning robust. Since non-rehearsal-based methods do not perform well when performing adversarial training, we adapted the rehearsal-based method as the baseline. *All implementation details are contained in supplementary material.*

4.2 Main results

We present an in-depth assessment of our proposed method with other adversarially trained CIL methods with different buffer sizes in Table 1 and Table 2. The results strongly demonstrate the superiority of our proposed method over other adversarially trained CIL methods across almost all scenarios. In buffer size of 2,000, our method achieved auto attack accuracy that is 5.99%p, 5.27%p, and 3.90%p

higher on average than the baseline on S-CIFAR10, S-SICFAR100, and S-TinyImageNet, respectively. Of particular interest is the measure of R-BWT in our method, which outperforms all other methods. This significantly higher R-BWT means that our method improves forgetting resistance, even with tiny buffer size scenarios. In addition, we can see that not only robust performance but also clean accuracy is the best in S-CIFAR100 and S-TinyImageNet.

4.3 Ablation studies

We study ablation studies to answer the following questions: **(Q1)** What about other adversarial training methods for ARCIL? **(Q2)** Do adversarial images play an essential role in maintaining flatness? **(Q3)** Do KL loss is sufficient to transfer the flatness of the previous model? **(Q4)** What is the effect of each proposed term? All ablation studies are experimented on ARCIL setting with a 2,000 buffer size on ResNet-18 with S-CIFAR100. *More detailed experimental settings and additional results are in the supplementary materials.*

Comparison with other AT methods (Q1)

Dataset	Buffer Size Method	2000				4000			
		Clean	PGD	AA	R-BWT	Clean	PGD	AA	R-BWT
S-TinyImageNet	FT w/ Buffer	6.80	3.07	2.80	-31.11	6.79	2.96	2.71	-30.61
	R-ER	8.79	2.52	2.45	-22.01	10.93	2.67	2.61	-21.08
	R-ER-ACE	18.05	1.59	1.41	-13.63	22.15	2.47	2.32	-12.82
	R-DER	6.90	2.85	2.27	-29.17	6.69	2.99	2.43	-28.86
	R-DER++	10.39	2.79	2.42	-22.94	13.61	3.18	2.76	-21.01
	R-iCaRL	19.32	5.25	3.33	-21.63	19.27	5.59	3.59	-21.40
	R-LUCIR	8.40	2.81	2.58	-26.81	15.11	2.67	2.03	-21.22
	Ours	27.59	10.17	6.37	-8.99	26.23	10.21	6.13	-9.97

Table 2: Adversarial training results on S-TinyImageNet. We measure Clean, PGD, Autoattack accuracy (%), and Robust BWT. Due to the significant catastrophic forgetting observed in small buffer sizes on S-TinyImageNet, we have selected relatively larger buffer sizes of 2,000 and 4000.

Method	Clean	PGD	R-BWT	R-LA
TRADES ($\lambda = 6$)	17.79	8.84	-39.16	44.35
TRADES ($\lambda = 1$)	21.89	8.29	-31.07	36.25
MART ($\lambda = 5$)	20.20	8.17	-34.93	39.61
MART ($\lambda = 1$)	20.56	7.91	-34.23	38.72
PGD-AT	34.13	10.78	-21.73	30.34

Method	Clean	PGD	BWT	R-BWT
None	34.18	10.62	-34.28	-21.49
Gaussian	36.30	11.68	-29.81	-19.44
Uniform	36.91	12.26	-27.12	-18.00
PGD	39.19	15.92	-10.96	-8.28

Table 3: Performance over different adversarial training methods.

When integrating adversarial training into CIL, we have the flexibility to incorporate alternative adversarial training methods, such as TRADES[49] and MART[45] rather than PGD-AT[33]. Since TRADES and MART usually perform better than PGD-AT and are widely used for the baseline for adversarial training, we selected TRADES and MART. However, in Fig. 6, PGD-AT achieves higher clean and robust accuracy compared to TRADES and MART. All the adversarial training methods achieve similar clean and robust accuracy in the first task, but TRADES and MART forget their previous tasks more than the PGD-AT method does with the increase in tasks. Table 3 shows that while TRADES and MART have better learning accuracy than PGD-AT, their clean and robust accuracy are lower due to significant forgetting. In addition, as the regularization term gets weaker (when $\lambda = 1$), forgetting is alleviated and learning accuracy decreases. This indicates that TRADES and MART’s strong consistency

Table 4: Adversarial training results with different methods for generating perturbation for FPD. We utilized the maximum norm bounded $\epsilon_\infty = 8/255$. ‘None’ indicates FPD with zero perturbation, *i.e.*, utilizing only adversarial distillation.

constraints between clean and adversarial images of the current task hinder knowledge retention of past tasks. Therefore, we incorporate PGD-AT for AR-CIL.

Analysis on δ of FPD in Eq. (8) (Q2)

In Fig. 1, one might think random noise can also benefit maintaining flatness. Thus, we experiment with random noise to see if adversarial perturbation indeed helps maintain flatness rather than random noise. In Table 4, we observe that even the application of Gaussian or uniform distribution for the δ of FPD loss effectively reduces both the BWT and R-BWT. However, we can see that the results are the best when PGD is used for FPD loss. This implies that FPD can flatten the loss surface even with random perturbations, but the most optimal outcomes

Method	Clean	PGD	BWT	R-BWT	LA	R-LA
L1	38.57	15.86	-11.87	-8.74	49.25	23.73
L2(MSE)	39.27	15.57	-14.23	-10.22	52.08	24.77
IKL	36.81	16.01	-9.59	-6.70	45.44	22.04
KL	39.20	15.80	-11.39	-8.18	49.45	23.16

Table 5: Adversarial training results on different surrogate losses for FPD. KL loss is selected to prevent biases towards one side in both forgetting and learning, achieving high robust and clean accuracy simultaneously.

are achieved with adversarial perturbations.

Furthermore, the left plot in Fig. 7 illustrates the impact of varying perturbation sizes of FGSM[18] in FPD. Notably, larger perturbation sizes led to lower gradient and curvature norms. Moreover, the right plot in Fig. 7 demonstrates that the gradient and curvature are unrelated to the number of iteration steps used in the PGD attack. In summary, FPD favors adversarial images with larger perturbation sizes, irrespective of the number of PGD steps. Thus, we apply the already generated PGD-attacked image for training model with FPD.

Surrogate loss for transferring flatness (Q3)

For the surrogate loss of D in Eq. (11), we conducted experiments using various loss functions, as summarized in Table 5. The L1 and L2 exhibited relatively weaker resistance to forgetting, leading to sub-optimal performance. On the other hand, the Improved KL (IKL)[11] loss, which reformulates the

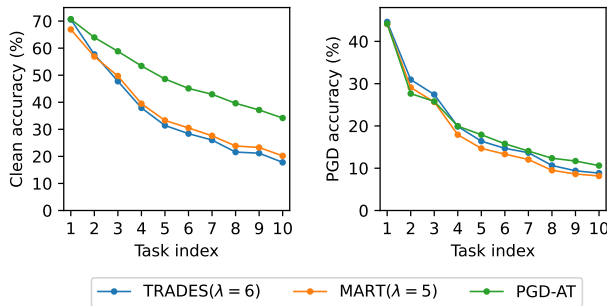


Figure 6: The clean and PGD accuracy of various adversarial training methods to the incremental task steps.

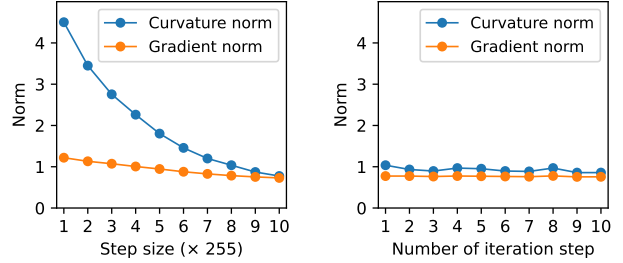


Figure 7: The gradient and curvature norm according to the step size of the FGSM attack with FPD. (Left) The gradient and curvature norm according to iteration step number of PGD attack ($\epsilon_\infty = 8/255$) with FPD. (Right)

loss	Clean	PGD	R-BWT	R-LA
L_{AD}	34.89	10.78	-20.50	29.23
L_{LAD}	35.27	11.15	-20.54	30.54
$L_{AD} + L_{FPD}$	39.19	15.92	-7.68	22.82
$L_{LAD} + L_{FPD}$	39.44	16.59	-9.74	25.36

Table 6: Impact of each component on our method.

KL divergence into an intense distillation loss, resulted in lower learning accuracy and reduced accuracy on clean images. After careful analysis, we ultimately select the KL loss as the surrogate loss for FPD because it is balanced between resistance to forgetting and learning ability.

Effect of each components of our method (Q4)

In Table 6, we conducted experiments on each component of the proposed method. Comparing L_{AD} and $L_{AD} + L_{FPD}$, we can see that the performance improves significantly when L_{FPD} is added. Although the learning accuracy is reduced when we add L_{FPD} , this is compensated for by L_{LAD} . Notably, replacing L_{AD} with L_{LAD} in the second and fourth rows of Table 6 results in improved learning accuracy and overall performance.

5 Conclusion

We have proposed a novel FPD loss and LAD loss in ARCIL setting. We observe that adversarially

trained models face the flatness forgetting problem upon encountering new tasks. From this observation, we distill output difference from a previous task model to preserve flatness and thus conserve robustness effectively. Additionally, when new tasks enter the model, we modify the model’s logits and then distill these logits into the model to better adapt to new tasks. We achieve state-of-the-art performance in incremental learning setups with adversarial robustness, which provides a strong baseline in this field. Additionally, because our study raises the problem of flatness forgetting problem for the first time, it provides a new perspective on feature learning in adversarial training.

References

- [1] Rahaf Aljundi, Min Lin, Baptiste Goujaud, and Yoshua Bengio. Gradient based sample selection for online continual learning. *Advances in neural information processing systems*, 32, 2019. 4
- [2] Zeyuan Allen-Zhu and Yuanzhi Li. Feature purification: How adversarial training performs robust deep learning. In *2021 IEEE 62nd Annual Symposium on Foundations of Computer Science (FOCS)*, pages 977–988. IEEE, 2022. 1
- [3] Anish Athalye, Nicholas Carlini, and David Wagner. Obfuscated gradients give a false sense of security: Circumventing defenses to adversarial examples. In *International conference on machine learning*, pages 274–283. PMLR, 2018. 1
- [4] Tao Bai, Chen Chen, Lingjuan Lyu, Jun Zhao, and Bihan Wen. Towards adversarially robust continual learning. In *ICASSP 2023-2023 IEEE International Conference on Acoustics, Speech and Signal Processing (ICASSP)*, pages 1–5. IEEE, 2023. 4
- [5] Yang Bai, Xin Yan, Yong Jiang, Shu-Tao Xia, and Yisen Wang. Clustering effect of adversarial robust models. *Advances in Neural Information Processing Systems*, 34:29590–29601, 2021. 1
- [6] Yang Bai, Yuyuan Zeng, Yong Jiang, Shu-Tao Xia, Xingjun Ma, and Yisen Wang. Improving adversarial robustness via channel-wise activation suppressing. *arXiv preprint arXiv:2103.08307*, 2021. 1, 2
- [7] Matteo Boschini, Lorenzo Bonicelli, Pietro Buzzega, Angelo Porrello, and Simone Calderara. Class-incremental continual learning into the extended der-
- verse. *IEEE Transactions on Pattern Analysis and Machine Intelligence*, 45(5):5497–5512, 2022. 4
- [8] Pietro Buzzega, Matteo Boschini, Angelo Porrello, Davide Abati, and SIMONE CALDERARA. Dark experience for general continual learning: a strong, simple baseline. In H. Larochelle, M. Ranzato, R. Hadsell, M.F. Balcan, and H. Lin, editors, *Advances in Neural Information Processing Systems*, volume 33, pages 15920–15930. Curran Associates, Inc., 2020. 2, 4, 8
- [9] Lucas Caccia, Rahaf Aljundi, Nader Asadi, Tinne Tuytelaars, Joelle Pineau, and Eugene Belilovsky. New insights on reducing abrupt representation change in online continual learning. *arXiv preprint arXiv:2104.05025*, 2021. 4, 8
- [10] Francesco Croce and Matthias Hein. Reliable evaluation of adversarial robustness with an ensemble of diverse parameter-free attacks. In *International conference on machine learning*, pages 2206–2216. PMLR, 2020. 7
- [11] Jiequan Cui, Zhuotao Tian, Zhisheng Zhong, Xiaojuan Qi, Bei Yu, and Hanwang Zhang. Decoupled kullback-leibler divergence loss. *arXiv preprint arXiv:2305.13948*, 2023. 10
- [12] Zhun Deng, Linjun Zhang, Kailas Vodrahalli, Kenji Kawaguchi, and James Y Zou. Adversarial training helps transfer learning via better representations. *Advances in Neural Information Processing Systems*, 34:25179–25191, 2021. 1
- [13] Arthur Douillard, Matthieu Cord, Charles Ollion, Thomas Robert, and Eduardo Valle. Podnet: Pooled outputs distillation for small-tasks incremental learning. In *Computer Vision–ECCV 2020: 16th European Conference, Glasgow, UK, August 23–28, 2020, Proceedings, Part XX 16*, pages 86–102. Springer, 2020. 2, 6
- [14] Logan Engstrom, Andrew Ilyas, Shibani Santurkar, Dimitris Tsipras, Brandon Tran, and Aleksander Madry. Adversarial robustness as a prior for learned representations. *arXiv preprint arXiv:1906.00945*, 2019. 1
- [15] Sebastian Farquhar and Yarin Gal. Towards robust evaluations of continual learning. *arXiv preprint arXiv:1805.09733*, 2018. 4
- [16] Micah Goldblum, Liam Fowl, Soheil Feizi, and Tom Goldstein. Adversarially robust distillation. In *Proceedings of the AAAI Conference on Artificial Intelligence*, volume 34, pages 3996–4003, 2020. 3, 6
- [17] Ian J Goodfellow, Mehdi Mirza, Da Xiao, Aaron Courville, and Yoshua Bengio. An empirical investi-

- gation of catastrophic forgetting in gradient-based neural networks. *arXiv preprint arXiv:1312.6211*, 2013. 2, 3
- [18] Ian J Goodfellow, Jonathon Shlens, and Christian Szegedy. Explaining and harnessing adversarial examples. *arXiv preprint arXiv:1412.6572*, 2014. 10
- [19] Kaiming He, Xiangyu Zhang, Shaoqing Ren, and Jian Sun. Deep residual learning for image recognition. In *Proceedings of the IEEE conference on computer vision and pattern recognition*, pages 770–778, 2016. 7
- [20] Saihui Hou, Xinyu Pan, Chen Change Loy, Zilei Wang, and Dahua Lin. Learning a unified classifier incrementally via rebalancing. In *Proceedings of the IEEE/CVF conference on computer vision and pattern recognition*, pages 831–839, 2019. 2, 4, 8
- [21] Bo Huang, Mingyang Chen, Yi Wang, Junda Lu, Minhao Cheng, and Wei Wang. Boosting accuracy and robustness of student models via adaptive adversarial distillation. In *Proceedings of the IEEE/CVF Conference on Computer Vision and Pattern Recognition*, pages 24668–24677, 2023. 3
- [22] Andrew Ilyas, Shibani Santurkar, Dimitris Tsipras, Logan Engstrom, Brandon Tran, and Aleksander Madry. Adversarial examples are not bugs, they are features. *Advances in neural information processing systems*, 32, 2019. 2, 6
- [23] Gaojie Jin, Xiping Yi, Wei Huang, Sven Schewe, and Xiaowei Huang. Enhancing adversarial training with second-order statistics of weights. In *Proceedings of the IEEE/CVF Conference on Computer Vision and Pattern Recognition*, pages 15273–15283, 2022. 1
- [24] Minsoo Kang, Jaeyoo Park, and Bohyung Han. Class-incremental learning by knowledge distillation with adaptive feature consolidation. In *Proceedings of the IEEE/CVF conference on computer vision and pattern recognition*, pages 16071–16080, 2022. 2, 6
- [25] Junho Kim, Byung-Kwan Lee, and Yong Man Ro. Distilling robust and non-robust features in adversarial examples by information bottleneck. *Advances in Neural Information Processing Systems*, 34:17148–17159, 2021. 6
- [26] Klim Kireev, Maksym Andriushchenko, and Nicolas Flammarion. On the effectiveness of adversarial training against common corruptions. In *Uncertainty in Artificial Intelligence*, pages 1012–1021. PMLR, 2022. 1
- [27] James Kirkpatrick, Razvan Pascanu, Neil Rabinowitz, Joel Veness, Guillaume Desjardins, Andrei A Rusu, Kieran Milan, John Quan, Tiago Ramalho, Agnieszka Grabska-Barwinska, et al. Overcoming catastrophic forgetting in neural networks. *Proceedings of the national academy of sciences*, 114(13):3521–3526, 2017. 4
- [28] Alex Krizhevsky, Geoffrey Hinton, et al. Learning multiple layers of features from tiny images. 2009. 7
- [29] Ya Le and Xuan Yang. Tiny imagenet visual recognition challenge. *CS 231N*, 7(7):3, 2015. 7
- [30] Lin Li and Michael Spratling. Data augmentation alone can improve adversarial training. *arXiv preprint arXiv:2301.09879*, 2023. 3
- [31] Zhizhong Li and Derek Hoiem. Learning without forgetting. *IEEE transactions on pattern analysis and machine intelligence*, 40(12):2935–2947, 2017. 4
- [32] Divyam Madaan, Jinwoo Shin, and Sung Ju Hwang. Adversarial neural pruning with latent vulnerability suppression. In *International Conference on Machine Learning*, pages 6575–6585. PMLR, 2020. 6
- [33] Aleksander Madry, Aleksandar Makelov, Ludwig Schmidt, Dimitris Tsipras, and Adrian Vladu. Towards deep learning models resistant to adversarial attacks. *arXiv preprint arXiv:1706.06083*, 2017. 3, 9
- [34] Javier Maroto, Guillermo Ortiz-Jiménez, and Pascal Frossard. On the benefits of knowledge distillation for adversarial robustness. *CoRR*, abs/2203.07159, 2022. 3
- [35] Seyed-Mohsen Moosavi-Dezfooli, Alhussein Fawzi, Jonathan Uesato, and Pascal Frossard. Robustness via curvature regularization, and vice versa. In *Proceedings of the IEEE/CVF Conference on Computer Vision and Pattern Recognition*, pages 9078–9086, 2019. 2, 4
- [36] Chongli Qin, James Martens, Sven Gowal, Dilip Krishnan, Krishnamurthy Dvijotham, Alhussein Fawzi, Soham De, Robert Stanforth, and Pushmeet Kohli. Adversarial robustness through local linearization. *Advances in Neural Information Processing Systems*, 32, 2019. 2
- [37] Sylvestre-Alvise Rebuffi, Sven Gowal, Dan A Calian, Florian Stimberg, Olivia Wiles, and Timothy Mann. Fixing data augmentation to improve adversarial robustness. *arXiv preprint arXiv:2103.01946*, 2021. 3
- [38] Sylvestre-Alvise Rebuffi, Alexander Kolesnikov, Georg Sperl, and Christoph H Lampert. icarl: Incremental classifier and representation learning. In *Proceedings of the IEEE conference on Computer Vision and Pattern Recognition*, pages 2001–2010, 2017. 2, 4, 6, 8

- [39] Matthew Riemer, Ignacio Cases, Robert Ajemian, Miao Liu, Irina Rish, Yuhai Tu, and Gerald Tesauro. Learning to learn without forgetting by maximizing transfer and minimizing interference. *arXiv preprint arXiv:1810.11910*, 2018. [2](#), [4](#), [8](#)
- [40] Hadi Salman, Andrew Ilyas, Logan Engstrom, Ashish Kapoor, and Aleksander Madry. Do adversarially robust imagenet models transfer better? *Advances in Neural Information Processing Systems*, 33:3533–3545, 2020. [1](#)
- [41] Shibani Santurkar, Dimitris Tsipras, and Aleksander Madry. Breeds: Benchmarks for subpopulation shift. *arXiv preprint arXiv:2008.04859*, 2020. [1](#)
- [42] Jonathan Schwarz, Wojciech Czarnecki, Jelena Luketina, Agnieszka Grabska-Barwinska, Yee Whye Teh, Razvan Pascanu, and Raia Hadsell. Progress & compress: A scalable framework for continual learning. In *International conference on machine learning*, pages 4528–4537. PMLR, 2018. [4](#)
- [43] Jihoon Tack, Sihyun Yu, Jongheon Jeong, Minseon Kim, Sung Ju Hwang, and Jinwoo Shin. Consistency regularization for adversarial robustness. In *Proceedings of the AAAI Conference on Artificial Intelligence*, volume 36, pages 8414–8422, 2022. [1](#)
- [44] Yisen Wang, Xingjun Ma, James Bailey, Jinfeng Yi, Bowen Zhou, and Quanquan Gu. On the convergence and robustness of adversarial training. *arXiv preprint arXiv:2112.08304*, 2021. [1](#)
- [45] Yisen Wang, Difan Zou, Jinfeng Yi, James Bailey, Xingjun Ma, and Quanquan Gu. Improving adversarial robustness requires revisiting misclassified examples. In *International Conference on Learning Representations*, 2020. [3](#), [9](#)
- [46] Boxi Wu, Jinghui Chen, Deng Cai, Xiaofei He, and Quanquan Gu. Do wider neural networks really help adversarial robustness? *Advances in Neural Information Processing Systems*, 34:7054–7067, 2021. [1](#)
- [47] Dongxian Wu, Shu-Tao Xia, and Yisen Wang. Adversarial weight perturbation helps robust generalization. *Advances in Neural Information Processing Systems*, 33:2958–2969, 2020. [1](#)
- [48] Friedemann Zenke, Ben Poole, and Surya Ganguli. Continual learning through synaptic intelligence. In *International conference on machine learning*, pages 3987–3995. PMLR, 2017. [4](#)
- [49] Hongyang Zhang, Yaodong Yu, Jiantao Jiao, Eric Xing, Laurent El Ghaoui, and Michael Jordan. Theoretically principled trade-off between robustness and accuracy. In *International conference on machine learning*, pages 7472–7482. PMLR, 2019. [3](#), [9](#)
- [50] Dawei Zhou, Nannan Wang, Bo Han, and Tongliang Liu. Modeling adversarial noise for adversarial training. In *International Conference on Machine Learning*, pages 27353–27366. PMLR, 2022. [1](#)
- [51] Jianing Zhu, Jiangchao Yao, Bo Han, Jingfeng Zhang, Tongliang Liu, Gang Niu, Jingren Zhou, Jianliang Xu, and Hongxia Yang. Reliable adversarial distillation with unreliable teachers. *arXiv preprint arXiv:2106.04928*, 2021. [3](#), [6](#)
- [52] Bojia Zi, Shihao Zhao, Xingjun Ma, and Yu-Gang Jiang. Revisiting adversarial robustness distillation: Robust soft labels make student better. In *Proceedings of the IEEE/CVF International Conference on Computer Vision*, pages 16443–16452, 2021. [3](#), [6](#)